Separation Science and Technology
Publication details, including instructions for authors and subscription information:
http://www.informaworld.com/smpp/title~content=t713708471

The Performance of a Rotating Module in Oily Emulsions Ultrafiltration

Fernando Vigo[a]; Claudio Uliana[a]; Paolo Lupino[a]
[a] INSTITUTE OF INDUSTRIAL CHEMISTRY OF THE UNIVERSITY OF GENOA, GENOA, ITALY

To cite this Article Vigo, Fernando , Uliana, Claudio and Lupino, Paolo(1985) 'The Performance of a Rotating Module in Oily Emulsions Ultrafiltration', Separation Science and Technology, 20: 2, 213 — 230
To link to this Article: DOI: 10.1080/01496398508058361
URL: http://dx.doi.org/10.1080/01496398508058361

SEPARATION SCIENCE AND TECHNOLOGY, 20(2 & 3), pp. 213-230, 1985

The Performance of a Rotating Module in Oily Emulsions Ultrafiltration

FERNANDO VIGO, CLAUDIO ULIANA, and PAOLO LUPINO

INSTITUTE OF INDUSTRIAL CHEMISTRY OF THE UNIVERSITY OF GENOA
GENOA, ITALY

Abstract

The rotating ultrafiltration module has been applied to concentrated oily emulsions with the aim of checking its practical features. The ultrafiltration yield has been measured as a function of pressure, tangential speed, temperature, oil concentration, and hydrodynamic conditions. An energy consumption evaluation has been performed and a comparison with tubular modules tried. The importance of turbulence promoters and the influence of the radial geometry of the module has been outlined by means of simulation tests with a transparent model system.

INTRODUCTION

The formation of boundary "gel" layers and the "fouling" phenomena during the ultrafiltration (U.F.) process are intimately connected problems. They have been studied by many research groups (*1–4*) whose results have led to the formulation of some theoretical models. As a general conclusion, it can be inferred that "gel layer" formation is the limiting factor, which can be reduced by proper setting of the hydrodynamic conditions during U.F.

This condition affects not only the energy consumption during the U.F. process, but also the module and system design. The two aspects are interconnected, as proper module design would reduce the energy consumption; however, commercial U.F. systems in use today are limited to four basic module designs (*4*): tubes, hollow fibers, flat plates, and spiral wound. All of them involve feed pumping at a rate sufficient to reach hydrodynamic conditions corresponding to an acceptable concentration polarization.

 0149-6395/85/2002-0213$3.50/0

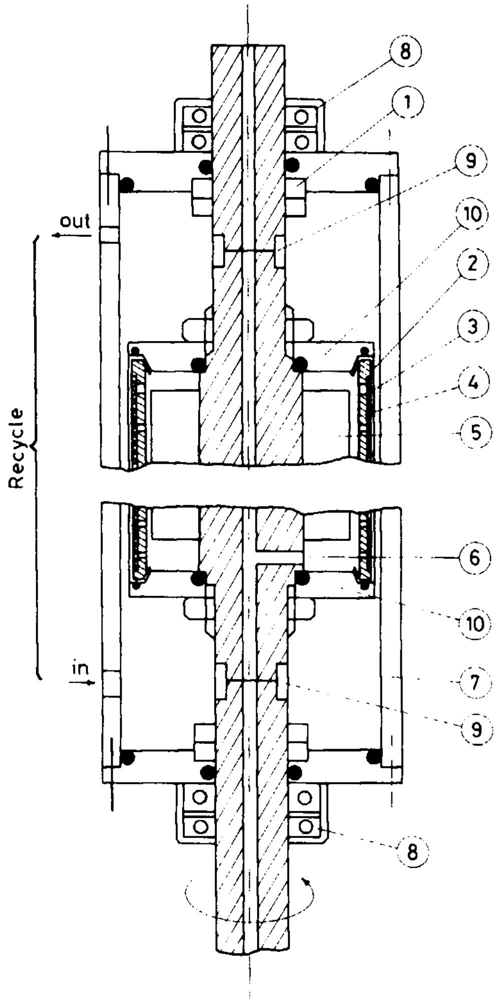

1	Mechanicals seals
2	Membrane
3	Membrane support
4	Inner cylinder
5	Expanded polystyrene filling
6	Collection hole
7	Outer shell
8	Bearings
9	Fast couplings
10	Membrane sealing

FIG. 1. Rotating U.F. module.

Only recently (*5*) has the application of the "rotative module" concept (*6*) to ultrafiltration been proposed. Many kinds of devices have been produced in order to obtain good rotative modules capable of reducing the concentration polarization by means of high shear stress flows: rotating bundles, disks, drums, etc.; in our opinion, the cylindrical device is the best compromise. In this type of module a cylindrical membrane moves concentric to a shell; its angular velocity, the gap between the membrane and the shell, as well as the characteristics of the inner surface of the shell can be varied in order to optimize the hydrodynamic conditions.

This situation is similar to that met in thin channel-flat modules, but the high shear stress conditions are here reached in a different way: this is also due to the Taylor vortex flow (*7*) which is typical of fluids inserted between two rotating cylinders. This type of module has already been used to study (*8, 9*) the mass transfer coefficient variations, i.e., the concentration polarization during the U.F. of different solutions (bovine seralbumin, dextrane, milk, etc.).

The purpose of our work was to verify the features of the rotative cylindrical module in industrial pollution abatement problems (in the present case, recovery of spent cutting oil emulsion) in order to evaluate the best performances and the energy consumption per ton of permeate, as well as to compare these characteristics with those obtained from the usual commercial systems (e.g., tubular devices).

EXPERIMENTAL MODULE

Our experiments were carried out with a cylindrical module. It was assembled on the basis of previous tests suggestions (*9*) with the aim of obtaining: (a) improved yields by reducing energy losses due to mechanical friction, and (b) a device capable of providing suitable information on the applicability of such modules to the recovery of oils from spent industrial emulsions. A cylindrical rotational module can be assembled in two different configurations: the first locates the membrane on the inner wall of a rotating drum and the second puts the membrane on the outer surface.

The second type of module was chosen and realized as described by Fig. 1.

The module was entirely made of steel. The rotating seals were the usual centrifuge pump sealings, and thrust bearings were utilized. The inner surface of the shell was lined with an extractable jacket. Thus, by changing it we could vary the annular space around the membrane and the roughness characteristics of the wall as well. The inside of the drum bearing the membrane was filled with annular sections of expanded polystyrene in order to avoid permeate accumulation.

The main characteristics of the module were a follows: height 40 cm, diameter of the rotating membrane 10 cm, membrane area 700 cm^2, gap between the membrane and the wall of the shell varying from 2.5 to 3.3 mm.

The main characteristics of the module were as follows: height 40 cm, (Celgard 3500 by Celanese). It was formed in the shape of a cylinder by thermal welding it to a support made of nonwoven nylon fibers. The tube so obtained was then slipped around the rotating drum.

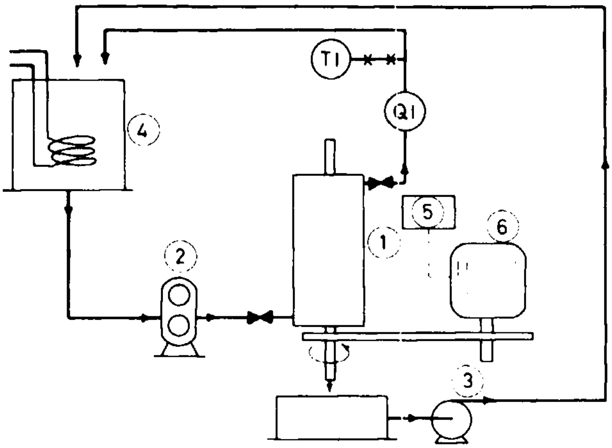

U.F. Circuit	
1 Rotanting module	4 Feed tank
2 Gear pump	5 Power meter
3 Permeate recycling pump	6 dc Electric motor

FIG. 2. U.F. circuit.

The two ends of the membrane tube were folded inward and sealed with an O-ring bearing disk (see Fig. 1). The whole drum was then easily inserted in the module by means of two self-centering fast couplings.

The module was driven by a 0.75-hp dc electric motor, and the oily emulsions were fed by means of a gear pump (see Fig. 2). The U.F. circuit could operate up to 800 kPa, with a tangential rotation speed up to 12 m/s. The temperature could be varied up to 70°C, and the recirculation rate was between 0 and 150 L/h. The power consumption was checked by means of voltage–current measurements, and the rotation speed was matched by an electronic device driven by a tachometer.

OILY EMULSIONS ULTRAFILTRATION

Experimental Data

The aforementioned U.F. circuit allowed us to investigate the ultrafiltration of freshly prepared emulsions of cutting oil.

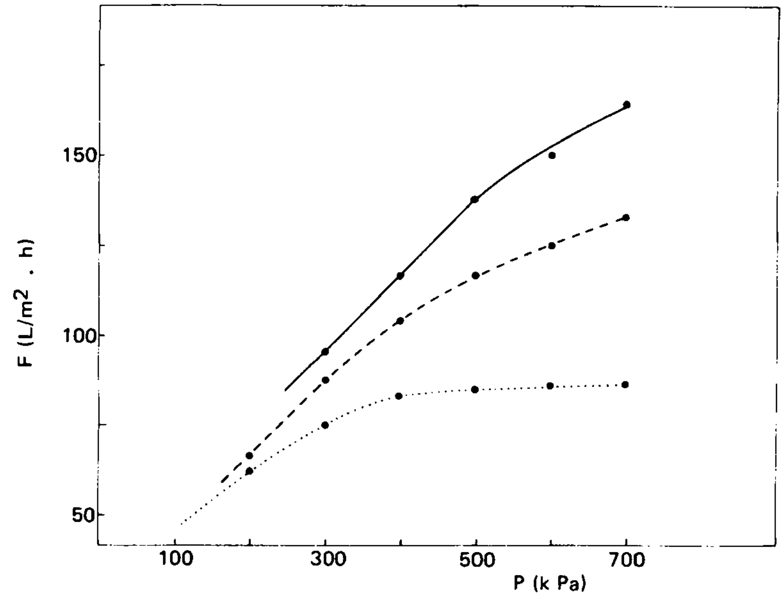

FIG. 3. Permeate flux F as a function of pressure P. Tangential speeds: 9 m/s (——), 7 m/s (- -), 5 m/s (· · ·).

The performances of the rotating module were recorded as functions of pressure, temperature, rotation speed, oil concentration, surface characteristics of the shell facing the membrane, and gap width between them.

Permeate flux, oil rejection, and energy consumed were measured during each test run.

In Fig. 3 the performances of the membrane as functions of the pressure at three different tangential speeds are reported. Oil concentration and the other conditions were kept constant. From the plot of Fig. 3 it can easily be inferred that both the pressure and the tangential velocity are highly effective in enhancing the permeate flux; that is, the specific effectiveness of the membrane. The result was obviously expected, considering the influence of such parameters on the mechanism of the ultrafiltration (*4, 6*). In the present situation, however, it must be emphasized once more that, while in systems based on total recirculation of the feed (as in tubular ones, for instance), pressure and velocity are connected through the head losses, in a rotative module they can be independently varied. This aspect is one of the most interesting features both from a practical and a theoretical point of view.

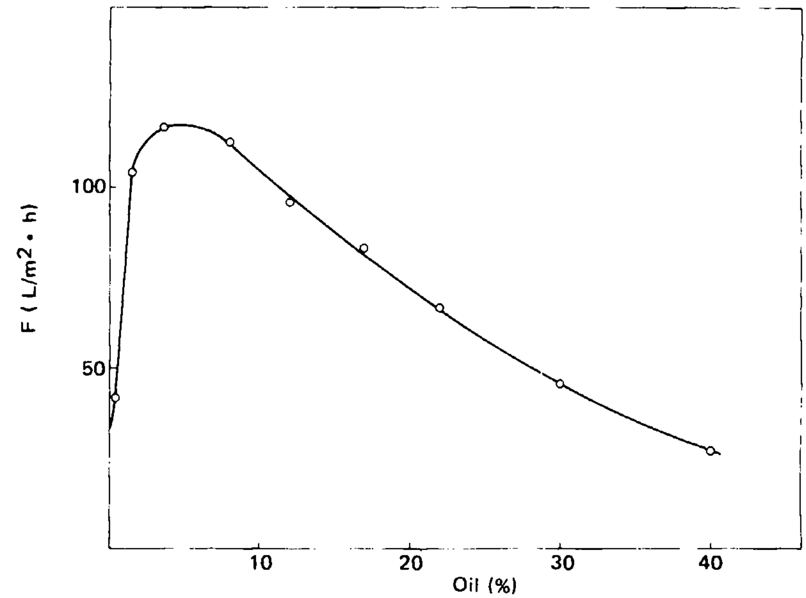

FIG. 4. Permeate flux F as a function of oil concentration.

This possibility has been successfully exploited by Hallström and Lopez-Leiva (*6–10*) for studying the mechanism of "gel layer" formation with proteins and milk.

Our main aim was focused on possible practical applications, and no specific study about gel layer build up was performed. In any case, some of our results fit quite well with the conclusions drawn by the aforementioned research groups.

The percent of retained oil, i.e., the rejection, was measured by solvent extraction of the permeate and infrared spectroscopy. Since we always found rejections higher than 99.9%, we do not report any plot showing detailed trends.

In Fig. 4 the permeate flux as a function of the oil concentration is reported. The trend is quite similar to that found in other cases (*11*). We attribute this behavior to the influence of emulsifying agents on the gel-layer characteristics.

The influence of temperature on the permeate flux, while keeping the oil concentration constant, was also investigated.

The evaluated slope of flux variation with temperature was equal to 1.46 $L/m^2 \cdot h \cdot {}^\circ C$. This value, in terms of percent, once more seems to be nearly

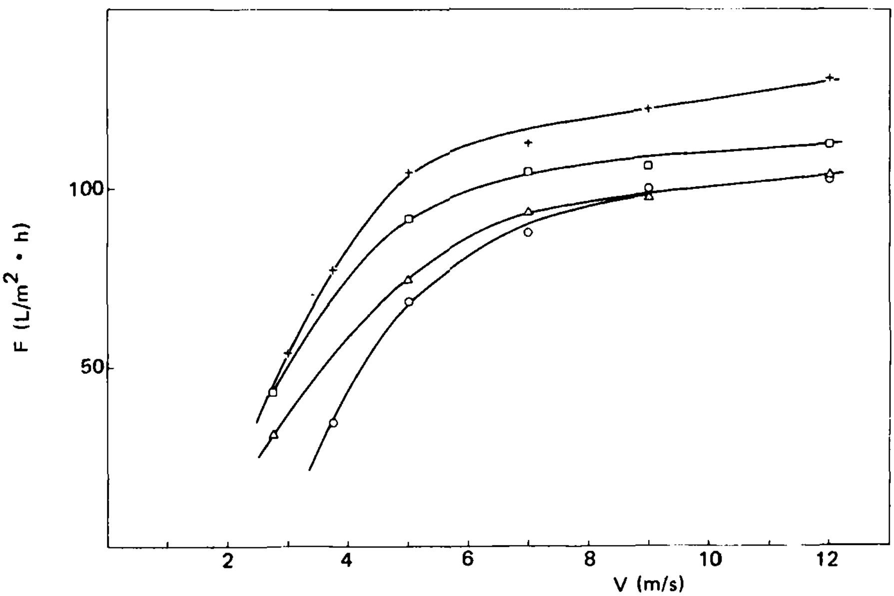

FIG. 5. Permeate flux F as a function of tangential speed (v). Gap width: 2.5 mm (Δ), 3.3 mm (O), 270 mesh net (gap 2.5) (+), 140 mesh net (gap 2.5) (□).

the same as that found by drawing a plot of the absolute viscosity of water as a function of temperature.

For the following experiments the standard conditions chosen were 20% oil and 40°C. All the data refer to the above conditions, if others are not declared.

In Fig. 5 the influence of the annular gap width around the membrane is shown. In spite of the small difference between the two gap values (2.5 and 3.3 mm), the behavior of the permeate flux seems to be sharply influenced. At lower rotation speeds this effect is more remarkable due to the different hydrodynamic conditions and to the different size of the Taylor vortices (see Appendix). This fact leads to a reduced value of the transport coefficient in the case of the 3.3 mm gap, which can also be seen from the well-known relation (*1*, *9*)

$$\mathrm{Sh} = kd/D = A\mathrm{Ta}^a\mathrm{Sc}^{1/3}$$

where A, a = constants

Ta = Taylor number
Sc = Schmidt number
Sh = Sherwood number
k = mass transfer coefficient
d = gap width
D = diffusion coefficient

In the same graph the influence of the roughness of the shell wall is also reported. Differences in roughness were obtained by means of nets of 270 and 140 mesh, respectively.

The effectiveness of the nets is clearly evident from the plots of the permeate flux; both curves are higher than the corresponding ones obtained with the same gap width (2.5 mm) but with a smooth wall.

This effect has been ascribed to an increase of the mass transfer coefficient due to the presence of nets acting as static convection promoters (*12, 13*). The 270 mesh net seems to be more effective than the 140 one, especially at higher rotational speeds. This fact is worthy of further investigations not only for technological purposes (*14*) but also in order to clarify the correct meaning of the flux plateau vs the rotation speed (*6*).

ENERGY CONSUMPTION EVALUATION

By considering the schematic drawing of the U.F. plant reported in Fig. 2, it is possible to identify the following sources of energy consumption:

(A) Pumping the feed through the module (by means of the gear pump)
(B) Bearings and sealings friction
(C) Shearing stress at the rotating membrane surface

Let us consider these points in more detail. The energy consumption of *type A* (E_a) can be evaluated by taking into account the working pressure and the feed delivery. In our opinion, the latter must be at least an order of magnitude greater than the permeate flux in order to avoid concentration build-up in the module. Starting from the well-known relationship for the calculation of the pumping power:

$$W = \frac{QPg\rho}{\eta \times 10^7}$$

where W is the power (kW)
Q is the pump delivery (L/s)
P is the pressure (kPa)
g is the gravity constant (m/s^2)
ρ is the density of the feed (kg/m^3)
η is the pump yield

We can also write, in the case of a module having 1 m^2 of membrane (if $\rho = 1000$ and $\eta = 0.5$),

$$W = \frac{FPg}{1000}\,\frac{\rho \times 10^{-3}}{3600} = 5.4 \times 10^{-6} FP$$

where F is the permeate flux (L/m$^2 \cdot$ h) or, more directly,

$$E_a = 5.4 \times 10^{-3} P \qquad \text{(kWh/m}^3\text{ of permeate)}$$

Energy consumption of *type B* (E_b) is due to the friction of the sealings and the bearings; this energy loss is fairly independent of the size of the module if the axis diameter of the drum is kept constant.

An evaluation of the energy loss can be made on the basis of the supplier's data; nevertheless, we preferred to evaluate it through experimental tests. This was achieved by running the module without the central drum and measuring the power absorption as a function of the pressure and the rotation speed. During the tests the module was filled with the oily emulsion (20% oil).

In Fig. 6 the data concerning the energy consumption at different pressures and speeds are reported.

The temperature influence is only slight, therefore, further experiments were run at 40°C. We consider a module having 1 m^2 of membrane, so that the energy loss can be written as E_b = kWh/m^3, which is dimensionally homogeneous with E_a.

The energy losses due to shearing stress on the membrane are strictly related to the characteristics of the module (membrane surface, annular gap width, roughness) and, obviously, dependent on the working conditions. We tried to evaluate them experimentally by measuring the overall consumption of the rotating parts of the module; the bearing and sealings contributions were subtracted, and the value obtained was referred to a "standard" module having 1 m^2 of membrane area.

The energy consumption was evaluated as a function of pressure,

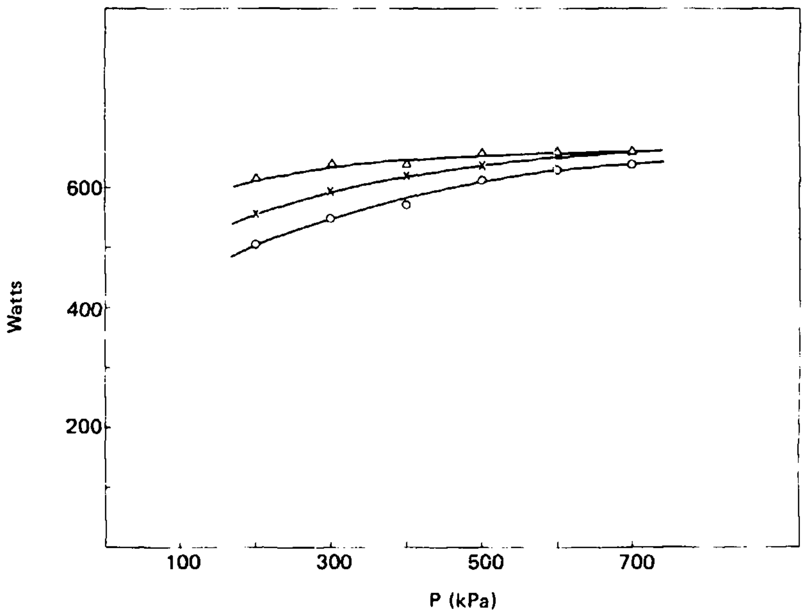

FIG. 6. Energy consumption at bearings and sealing as a function of pressure. Tangential speeds: 5 m/s (O), 7 m/s (×), 9 m/s (Δ).

rotation speed, annular gap width, and roughness of the shell wall; the data are reported in Figs. 7, 8, and 9 and are expressed as kWh/m^3 of permeate (E_c).

Figure 7 shows the influence of the pressure and rotation speed on E_c. In the same figure the plots obtained with different annular gap widths (dashed lines) are reported.

Figures 8 and 9 show the influence of the shell wall roughness.

In Fig. 10 the overall specific consumption of energy E_t, i.e., the sum of the values $E_a + E_b + E_c$, related to a module having 1 m^2 of membrane surface, is reported. The data deal with the case of smooth shell walls, but refer to two different annular gap widths. By comparing the values it is seen that narrow gaps and high rotation speeds are to be preferred.

Overall energy consumption in the presence of nets shows a quite different trend (see Fig. 11). Higher rotation speeds seem to be less advantageous, at least from the point of view of energy consumption; on the other hand, the nets have shown to be highly effective in enhancing the permeate productivity. The behavior of the plots in Fig. 11 can be interpreted as a compromise between the higher friction induced by the nets

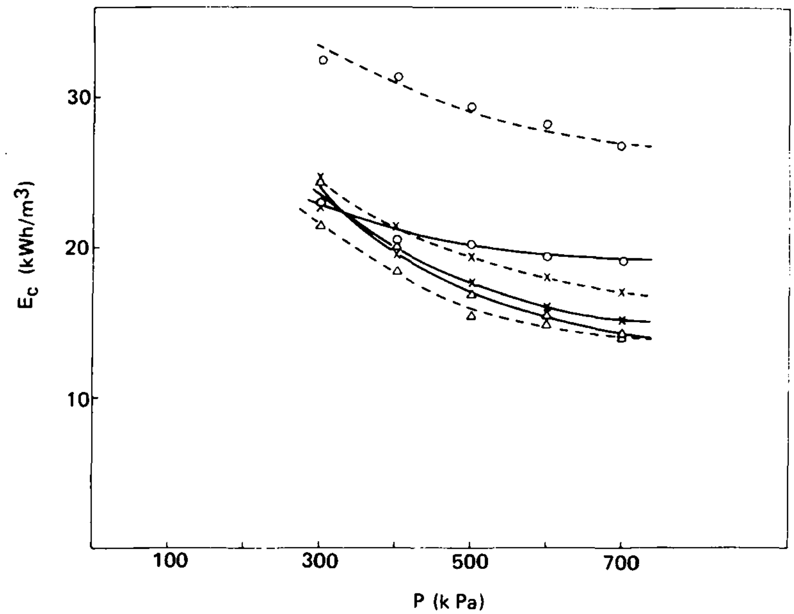

FIG. 7. Energy consumption E_c as a function of pressure. Tangential speed: 5 m/s (○), 7 m/s (×), 9 m/s (Δ). Annular gap width: 2.5 mm (———), 3.3 mm (- -).

and a better utilization of the energy consumed, especially at low rotation speeds.

CONCLUSIONS

Our investigation has provided some interesting data linked to the practical application of rotating modules to industrial processes, i.e., to the treatment of spent oily emulsions for recovery or pollution control purposes.

Our aim was to check the features of such modules when applied to highly demanding processes such as oily emulsions purification, as well as to compare their performances to those typical of commercial modules, e.g., tubular ones. We consider our results rather successful in this respect; the information obtained from experimental measurements and summarized in Table 1 allow us to consider the rotational module competitive to the tubular configuration.

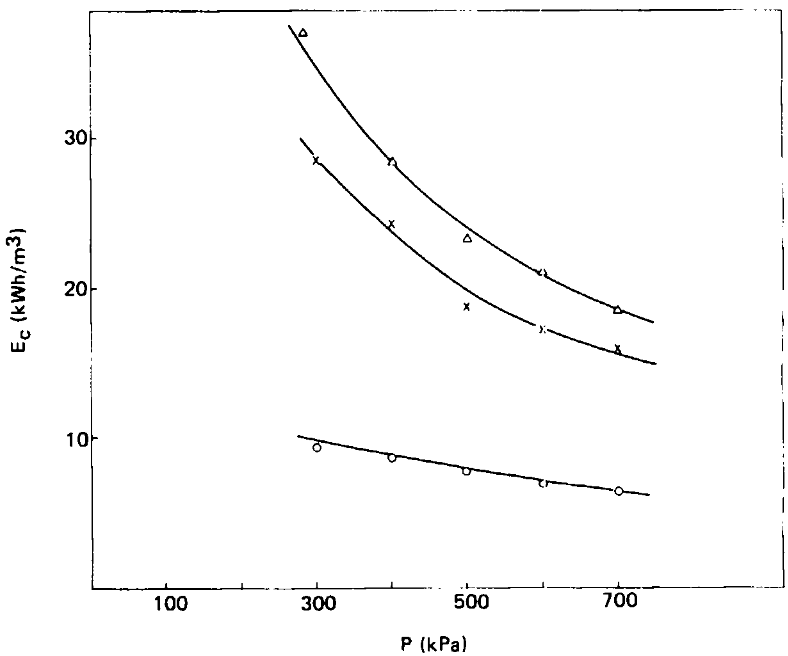

FIG. 8. Energy consumption E_c as a function of pressure in the presence of 270 mesh net. Tangential speed: 5 m/s (O), 7 m/s (×), 9 m/s (Δ).

All the data reported in Table 1 refer to the following working conditions: pressure 300 kPa, temperature 40°C, speed over the membrane 5 m/s, membrane area 1 m^2.

The data for the tubular system have been drawn from a plant having 8 modules 2-m long connected in series and powered by a 4-hp centrifuge pump. The tubular systems were fitted with the same type of membrane used in the rotating module.

Some other interesting features of the coaxial cylinders configuration must be pointed out: (a) it appears to be much more flexible than the tubular one; (b) the speed over the membrane and the pressure can be varied independently, thus reducing polarization by working at low pressure and high speed. This can be attained without changing the structure of the ultrafiltration loop, while that would be much more difficult or perhaps impossible in the case of tubular modules. (c) Finally, the rotating module is able to provide higher specific permeate fluxes, when required, in a much wider range than the tubular system. This characteristic

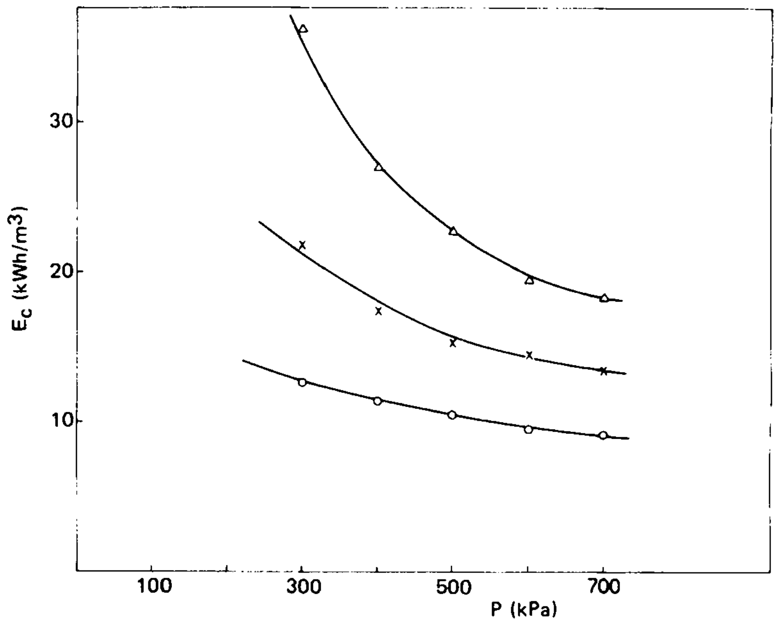

FIG. 9. Energy consumption E_c as a function of pressure in the presence of 140 mesh net. Tangential speed: 5 m/s (O), 7 m/s (×), 9 m/s (Δ).

permits dealing with smaller plants than the corresponding ones made of tubes.

APPENDIX

From the plot of Fig. 5 it clearly appears that the gap width d has a marked effect on membrane performance. This, of course, is due to different hydrodynamic conditions, i.e., to different Ta values. We notice, however, that in our case this fits only as a first approximation.

In fact, taking into account the above reported equation:

$$kd/D = A\mathrm{Ta}^a\mathrm{Sc}^{1/3}$$

we can also write

$$Fd = A'\mathrm{Ta}^a$$

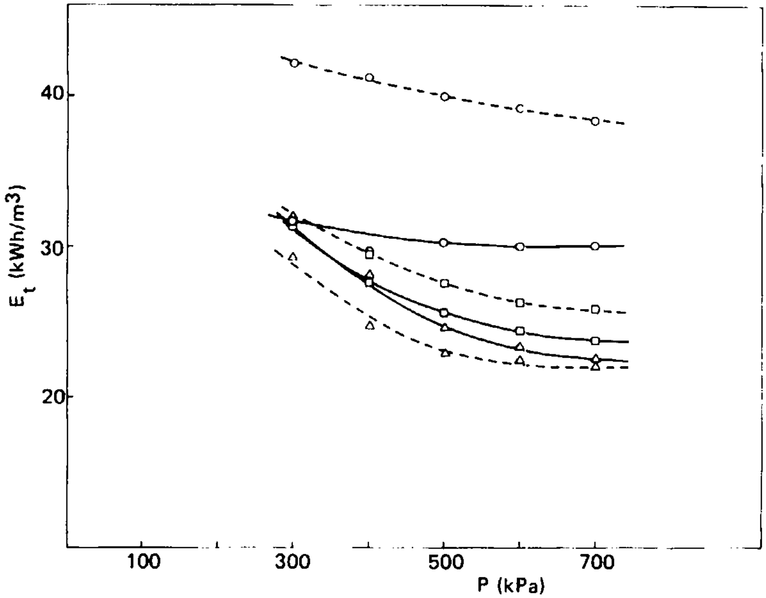

FIG. 10. Overall energy consumption E_t as a function of pressure. Tangential speed: 5 m/s (○), 7 m/s (□), 9 m/s (Δ). Annular gap width: 2.5 mm (——), 3.3 mm (- -).

where Ta has been calculated by

$$\sqrt{\mathrm{Ta}} = \frac{\omega R_i d}{\nu} \; \frac{\sqrt{d}}{\frac{d}{2} + R_i}$$

where R_i = inner cylinder radius (m)
ω = angular speed (rads/s)
ν = cinematic viscosity (m^2/s)

We report in Fig. 12 the values of *Fd* as a function of Ta for the case of 300 kPa.

All other conditions were kept constant, so that from the plot we can argue that, as expected, some other hydraulic parameters must affect the membrane permeability.

This fact stimulated us to investigate hydrodynamic phenomena on the membrane surface in more detail.

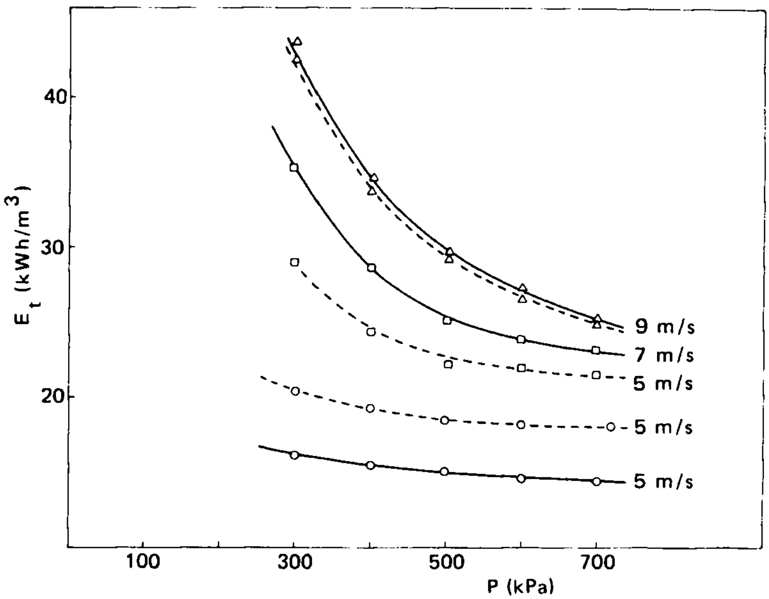

FIG. 11. Overall consumption E_t as a function of pressure in the presence of turbulence promotors: 270 mesh net (——) and 140 mesh net (- -).

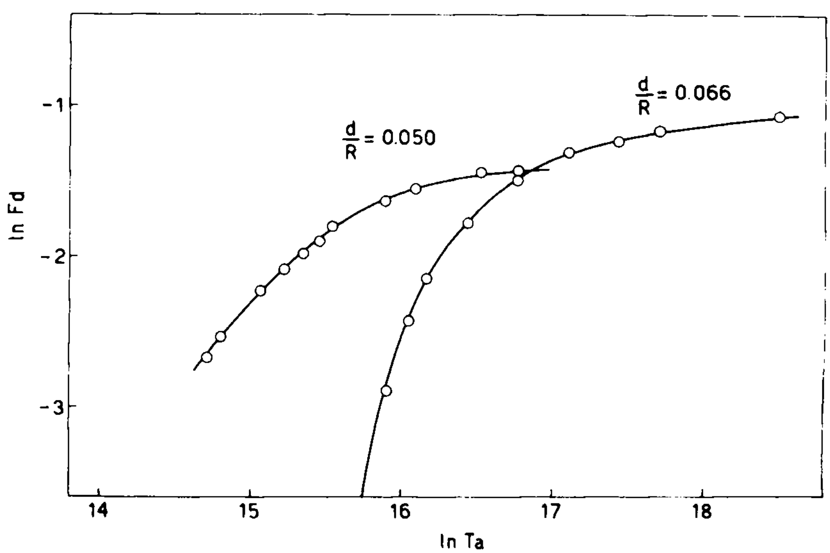

FIG. 12. Permeate flux F as a function of Ta values.

TABLE I

	Specific energy consumption (kWh/m^3 permeate)
Rotating: smooth wall, 2.5 mm gap	31.4
Rotating: smooth wall, 3.3 mm gap	42
Rotating: 270 mesh net, 2.5 mm gap	16.2
Tubular: 1 in. diameter	36

A completely transparent module was assembled having the same geometrical characteristics as the one used in our U.F. tests. By means of such a device we were able to follow the Taylor vortices formation and evolution as functions of tangential speed and gap width.

Many interesting perturbation modes were observed and photographically recorded with the aid of aluminum powder suspended in water.

The interpretation of the evolution of Taylor vortices is a hard task, even for experts active in this field (*15*). We limited our evaluation approach to the measure of the overall shape of the periodical perturbation in the same Ta range explored with the U.F. module.

In Fig. 13, photographs of the perturbations observed at three different gap widths and the same Ta value (obtained by adjusting the rotation speed) are reported. The apparent width of the vortices can be evaluated from these photographs. Note that in our Ta range they show elliptical rather than circular sections, and the main axis of the ellipse seems to be a function of the gap width. The following values were measured at constant Ta:

Gap width (mm)	Vortices width (mm)
1.5	3
2.5	4.5
3.5	6.1

For all cases represented in Fig. 13, an axial flow (0.2 m/s) was successively superimposed without any appreciable effect on the number and shape of the vortices.

These observations suggest that the shape of the vortices plays a role in membrane performance. Thus, it seems worth investigating whether a better U.F. yield can be achieved by proper shaping of the wall of the outer shell in a rotating module, avoiding at the same time the energy losses caused by rough turbulence promoters as in the case of nets.

We hope to report on this subject soon.

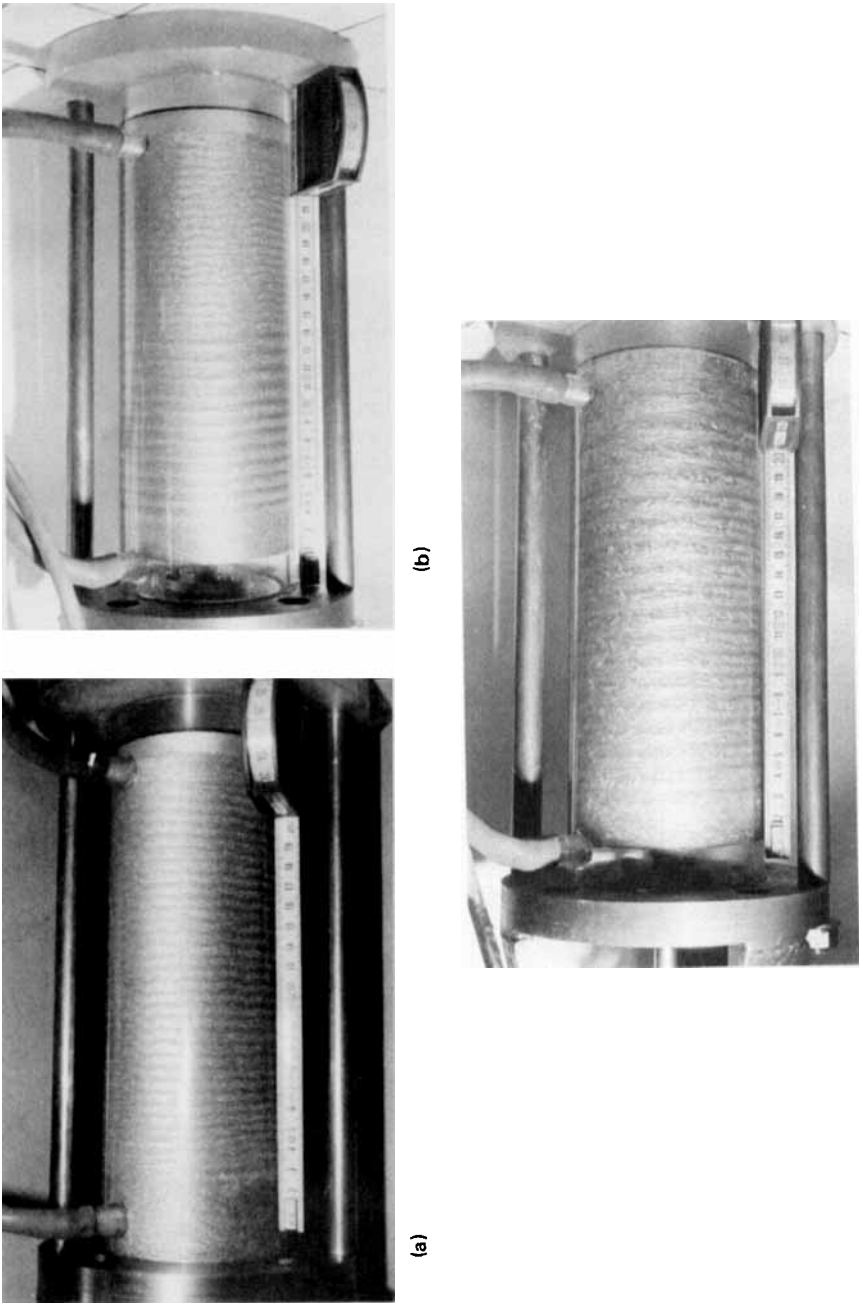

FIG. 13. Perturbation modes at different gap width values for $\sqrt{Ta} = 1000$. Gap width: 1.5 mm (a), 2.5 mm (b) (upper section of the photograph), 3.5 mm (c).

REFERENCES

1. S. Bruin, A. Kikkert, J. A. G. Weldring, and J. Hiddink, *Desalination, 35*, 223 (1980).
2. S. I. Nakao, T. Nomura, and S. Kimura, *AIChE J., 25*, 615 (1979).
3. A. S. Michaels, *Sep. Sci. Technol., 15*, 1305 (1980).
4. G. Belfort and F. Altena, *Desalination, 47*, 105 (1983).
5. H. K. Lonsdale, *J. M. Sci., 10*, 81 (1982).
6. M. Lopez-Leiva, *Desalination, 35*, 115 (1980).
7. G. I. Taylor, *Philos. Trans. R. Soc. London, A, 223*, 289 (1923).
8. T. K. Sherwood, P. L. T. Brian, and R. E. Fisher, *Ind. Eng. Chem., Fundam., 6*(1), 2 (1967).
9. M. Lopez-Leiva, "Ultrafiltration in Rotary Annular Flow," PhD Thesis, Lund University, Sweden, December 1979.
10. M. Lopez-Leiva, in *Polymer Science and Technology*, Vol. 13 (A. R. Cooper, ed.), Plenum, New York, 1980, p. 269.
11. F. Vigo, G. Capannelli, C. Uliana, and S. Munari, *Chim. Ind., 64*(2), 74 (1982).
12. J. Hiddink, D. Kloosterboer, and S. Bruin, *Desalination, 35*, 149 (1980).
13. Y. Winograd, A. Solan, and M. Toren, *Ibid., 13*, 171 (1973).
14. B. Hallström and M. Lopez-Leiva, *Deslination, 24*, 273 (1978).
15. D. Coles, *J. Fluid Mech., 21*, 385 (1965).

Received by editor September 18, 1984